Materials Science in Semiconductor Processing 66 (2017) 247–252

Contents lists available at ScienceDirect

Materials Science in Semiconductor Processing

journal homepage: www.elsevier.com/locate/mssp

Theoretical and experimental investigations of the thermoelectric properties of Al-, Bi- and Sn-doped ZnO

Weibao Guan, Liying Zhang, Chao Wang*, Yuanxu Wang*

Institute for Computational Materials Science, School of Physics and Electronics, Henan University, Kaifeng 475004, China

ARTICLE INFO

Keywords:
Thermoelectric oxide
ZnO
Dopant

ABSTRACT

In this paper, the thermoelectric properties of ZnO doped with Al, Bi and Sn were investigated by combining experimental and theoretical methods. The average Seebeck coefficient of Bi doped ZnO over the measured temperature range is improved from −90 to −497 μV/K. However, segregation of Bi_2O_3 in ZnO:Bi sample, confirmed by FESEM, lead to enormous grain growth and low electrical conductivity, which makes Bi is not a good dopant to improve *ZT* value of ZnO. As a 4+ valence cation, Sn doping actually show an increase in carrier concentration to 10^{20} cm^{-3}, further enhancing the electrical conductivity. Unfortunately, the Seebeck coefficient of ZnO:Sn samples is even lower than pure ZnO sample, which lead to a low *ZT* value. As for ZnO:Al sample, with nearly no change in lattice thermal conductivity, electrical conductivity and Seebeck coefficient were both enhanced. Threefold enhancement in *ZT* value has been achieved in ZnO:Al sample at 760 °C compared with pure ZnO.

1. Introduction

Nowadays, the development of renewable energy technology has become the subject of social development. Thermoelectric materials have been widely considered as a promising solution due to direct conversion of thermal energy into electrical energy. The efficiency of thermoelectric materials could be quantified by the dimensionless figure of merit *ZT*, $ZT = \sigma S^2 T/\kappa$, where *S* is Seebeck coefficient, σ is electric conductivity, κ is thermal conductivity and *T* is temperature. To achieve a high *ZT*, materials are required to have a low thermal conductivity κ, large values of Seebeck coefficient *S* as well as electrical conductivity σ [1]. Among the thermoelectric materials, ZnO has become a promising thermoelectric material due to its high Seebeck coefficient, low-cost production, potential high-temperature chemical stability and non-toxicity. Moreover, the investigations about the ternary compound ZnO indicates that it possess much better long-term stability in air at high temperature [2]. One of the most striking advantages of this new developed materials is its stability in air [3]. However, its practical applications are limited because ZnO exhibits a high resistivity and a high thermal conductivity. It was found that ZnO powder doped with various ions has improved electrical properties and other properties, therefore enlarging the potential technological applications of ZnO [4].

Although different element-doped ZnO were extensively studied [5–7], most of these research focused on electrical or optical properties of ZnO and few reports about thermoelectric properties of ZnO were presented. Ohtaki et al. first reported the thermoelectric properties of ZnO-based materials prepared by the solid-state reaction combined with normal sintering [8,9]. As mentioned above, ZnO materials possess high lattice thermal conductivity κ_L due to noncomplex wurtzite structure. Therefore, lowering κ_L will be essential to realize high *ZT* values in ZnO-based materials [10]. Recent investigations on ZnO ceramics show that their thermoelectric properties can be improved by substitution with aluminum or nickel [11]. It was reported that Al doping can lower κ_L by fostering grain refinement while at the same time tuning the carrier concentration to retain a high power factor (σS^2) [12]. For thermoelectric materials, heavy element doping is an effective way to reduce thermal conductivity [13,14]. Attempts at bismuth doping in ZnO leaded to very high Seebeck coefficient *S*, however, thermal conductivity κ has not been effectively decreased [10]. Another way to enhance the thermoelectric properties of ZnO is by tuning electrical conductivity and Seebeck coefficient. Research on the field of Sn doped ZnO shows that small amounts of tin substituting zinc atoms in ZnO lattice appear to cause a strong donor effect [15]. Sn serves as a doubly ionized donor impurity that providing carriers (electrons) will lead to a good quality ZnO based semiconductor [16]. In addition, Zn can be easily substituted by Sn and does not result in a large lattice distortion due to their almost equal radii [17]. However, there are few studies about the thermoelectric properties of Sn doping ZnO.

In this work, the thermoelectric properties of ZnO doped with Al, Bi

* Corresponding author.
E-mail addresses: wangchao@vip.henu.edu.cn (C. Wang), wangyx@vip.henu.edu.cn (Y. Wang).

http://dx.doi.org/10.1016/j.mssp.2017.03.027
Received 7 February 2017; Received in revised form 22 March 2017; Accepted 27 March 2017

and Sn were investigated by combining experimental and theoretical methods. According to our experimental results, Bi doping will dramatically increase the grain size of ZnO samples, which lead to higher lattice thermal conductivity. Boltzmann transport theory suggests that band structure and density of states can provide a general understanding of the thermoelectric performance. Here, differences of thermoelectric properties for Al, Bi and Sn doping ZnO due to electronic structure are analyzed by using first-principles calculations.

2. Experimental procedure and theoretical method

Four samples, pure ZnO, Al doped ZnO (ZnO:Al), Bi doped ZnO (ZnO:Bi) and Sn doped ZnO (ZnO:Sn), were prepared by a solid-state reaction method. The concentration of three dopants (Al, Bi and Sn) were all fixed at 2 wt%. Commercially available ZnO, Al_2O_3, Bi_2O_3 and SnO_2 powders each having a purity of 99% were used as starting materials. To obtain ideal samples, for each composition, the powders were mixed and ground in a ball mill with ethanol at speed of 320 revolution per minute for 24 h. The resulting mixtures were then dried at 80 °C in drying cabinet for 12 h. The dried powders were pressed into cylindrical pellets with a diameter of 12.7 mm at a pressure of 10 MPa. Then the pellets were sintered at 1000 °C for 48 h in air atmosphere using a tube furnace. After the sintering, the samples were ground again. The obtained powders were sintered using a SPS machine (SPS-211LX, Fuji Electronic Industrial Co. Ltd.) at 1000 °C for 5 min under uniaxial a pressure of 50 MPa in vacuum.

Crystal structure of the samples was characterized by X-ray diffraction (XRD, DX-2700, Dandong Fangyuan Instrument Co., Ltd.) with Cu K_α radiation accelerated in a 2θ range of 25–80°. The microstructure of the samples was observed by a field emission scanning electron microscope(FESEM, JSM-7001F, JEOL Co., Ltd.). Electrical conductivity and seebeck coefficient were measured using an static DC thermoelectric property measurement system (ZEM-3, ULVAC-RIKO, Inc.) under a low-pressure He atmosphere. Carrier concentration and mobility were analyzed at a temperature range of room temperature to 327 °C using DC Hall measurement system (ET9005, East Changing Technologies, Inc.) under a magnetic field of 1 T. The thermal conductivity was determined from the thermal diffusivity obtained by the laser flash method (DLF-1/EM1200, TA Inc.) in a Ar atmosphere.

The first-principles calculations on the atomistic relaxation and electronic structure of ZnO were performed using density functional theory (DFT) within projector augmented wave pseudopotentials as implemented in the VASP program package [18,19]. The exchange-correlation potential was dealed with form of the Perdew-Burke-Ernzerhof (PBE) generalized-gradient approximation (GGA) [20]. In our calculations, a $3\times3\times3$ supercell consisting of 54 Zn atoms and 54 O atoms was created. One dopant atom (Al, Bi, or Sn) replaced a Zn atom in the supercell to produce the doped ZnO. This corresponded to an impurity concentration of 1.85 at%. The plane-wave energy cutoff was chosen to be 400 eV and the tolerance in the selfconsistent field (SCF) calculation was 1×10^{-6} eV per atom. The Brillouin zone was sampled with a $7\times7\times5$ Monkhorst-Pack k-point grid. All chosen parameters have been tested and accepted due to the balance between the calculation accuracy and the time spent.

3. Results and discussion

Fig. 1 shows X-ray diffraction patterns of the pure ZnO, ZnO:Al, ZnO:Bi and ZnO:Sn samples. It can be seen that all strong peaks can be indexed as the pure hexagonal phase of wurtzite-type ZnO, which agrees well with the reported data (JCPDS No. 36–1451). No other impurity phases were detectable under the resolution of X-ray diffractometer with the additional doping of Al, Bi and Sn. However, the peaks of ZnO:Al, ZnO:Bi and ZnO:Sn samples related to the same plane are slightly shifted compared to pure ZnO samples. This behavior could be attributed to the difference between the ionic radius of Zn and the

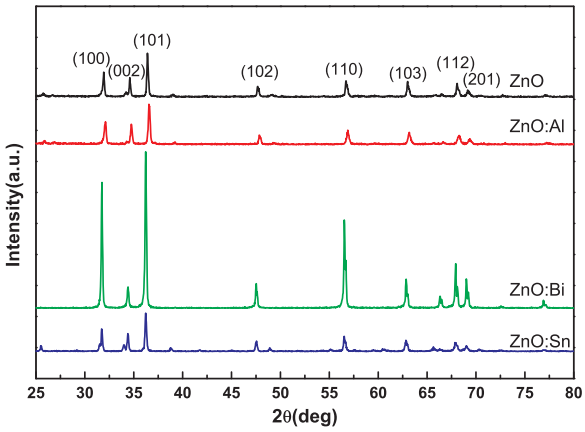

Fig. 1. XRD patterns for the pure ZnO, ZnO:Al, ZnO:Bi and ZnO:Sn samples.

dopant elements [21]. It is worth noting that the ZnO:Bi sample show relatively strong intensities of peaks in XRD pattern. The enhanced intensities in XRD peaks suggest better crystallinity in ZnO:Bi samples. As can be seen in Fig. 2, the relative intensity of (100), (101) peak in Bi-doped ZnO significantly enhanced. This means the texture happened in Bi-doped ZnO sample. To evaluate the degree of orientation of Bi doped ZnO, we calculated the volume fraction of pure ZnO and Bi doped ZnO. The volume fraction of (100) peak could be calculated using the following equation [22]:

$$\alpha_{100} = \sum (I_{n00}/I^*_{n00}) / \sum (I_{hkl}/I^*_{hkl}) \quad (1)$$

where I_{hkl} and I^*_{hkl} are measured intensity of the (*hkl*) peak, the intensity of the randomly oriented powders, respectively. The results of the degrees of orientation for pure ZnO and Bi-doped ZnO are 14%, 28.4% for (100) peak and 7%, 32.5% for (101) peak, respectively. The degrees of (100) and (101) for Bi doped samples are higher than that of pure ZnO. It reveals that the preferred orientation for ZnO:Bi is stronger.

SEM images of fracture surfaces of the pure ZnO, ZnO:Al, ZnO:Bi and ZnO:Sn samples are given in Fig. 2. As we can see from Fig. 2(a) and (b), for pure ZnO and ZnO:Al samples, the surfaces of grains were covered with nanoparticles. Additionally, it is clearly seen that there are large porous structures in these two samples. In contrast, the ZnO:Bi and ZnO:Sn samples were dense and the grains have clean surfaces. Particularly, from Fig. 2 (c) we could find that the grain growth is strongly enhanced with the addition of Bi, which is consistent with the XRD results. The grain size in ZnO:Bi sample is within range of from 2 to 6 μm and is far larger than that of other three samples. Similar phenomenon was also observed by Park et. al [2]. The reason can be well explained by the low solubility of Bi_2O_3 in ZnO. We can clearly see from the inset in Fig. 2(c) that some particles are segregated at grain boundaries. Park et. al. identified by XRD that these particles were α-Bi_2O_3 [2]. The non-detection of this phase in our XRD measurements is most likely due to its small amounts. The low-melting Bi_2O_3 at grain boundaries played a role in accelerating the mass transport of ZnO [10], which led to enormous grain growth in ZnO:Bi sample.

Fig. 3 shows temperature dependence of the electrical conductivity of ZnO, ZnO:Al, ZnO:Bi and ZnO:Sn samples. In order to clarify the origin of the difference in electrical conductivity, we also measured the carrier concentration and mobility as a function of temperature, as shown in Figs. 4 and 5, respectively. From Fig. 3, it is clearly seen that ZnO:Bi sample exhibits lower electrical conductivity over the entire measured temperature range from 100 °C to 760 °C, as compared to other three samples. As we mentioned before, the particles distributed at grain boundaries in ZnO:Bi sample are Bi_2O_3, which possesses a very high electrical resistivity ($> 10^8\Omega$ cm) [23]. The conduction mechanism of ZnO:Bi sample is a combination of electron hopping and tunneling between conductive grains and high-resistivity intergranular phase [24]. Additionally, the carrier concentration of ZnO:Bi sample is lower